Frequency Characteristics and Explanation of Notches Seen in Frequency Responses of Vehicles

Sittikorn Lapapong[*1], Alexander A. Brown[2], and Sean N. Brennan[2]

[1] National Metal and Materials Technology Center, 114 Thailand Science Park, Phahonyothin Rd., Klong 1, Klong Luang, Pathumthani 12120 Thailand

[2] Department of Mechanical and Nuclear Engineering, The Pennsylvania State University, 318 Leonhard Buidling, University Park, PA 16802 USA

*Corresponding Author: E-mail: sittikol@mtec.or.th, Tel: +66 2 564 6500 ext. 4758, Fax: +66 2 564 6332,

Abstract

The dynamics of vehicles has been widely studied since 1960s. Tremendous efforts have been spent to understand the dynamic behaviors of vehicle systems. Typically, the responses in the time domain and in the frequency domain are the primary validation techniques used to achieve this goal. In the experimental frequency characteristics of a vehicle, particularly the frequency responses from the front road-wheel steering angle to the lateral velocity, to the yaw rate, and to the roll rate, a unique characteristic similar to that of a notch filter can often be observed. Moreover, the cause of this characteristic is slightly known. Although high-order vehicle models can simulate this characteristic, there still is a need of a less-complex model to describe this characteristic. This work is the first effort to understand this characteristic through a low-order linear vehicle dynamic model. A vehicle dynamic model called the roll dynamic model is proposed in this work. Not only can the proposed model explain the cause of this notch characteristic, but also significantly improve the behavior matching to the experimental data once compared to the matching of the typical “bicycle model”.

Keywords*:* Vehicle, Vehicle Dynamics, Vehicle Modeling, Frequency Response

1. Introduction

In the past 40 years, there have been substantial attempts to develop and validate vehicle dynamic models. In effort to validate a vehicle model, there typically are two common schemes for comparing predicted and experimental results: time-domain matching and frequency-domain matching. Most of the validation work has been conducted in the time domain. However, since the time-domain technique typically relies on specific maneuvers such as J-turn, double-lane change, ramp steer etc., it may not reveal the dynamics within the frequency ranges of interest. Moreover, slight discrepancies between simulated and actual data may not seem severe in the time domain, but the differences become more defined once taken to the frequency domain, especially at higher frequencies [1]. This issue leads to a necessity of the frequency-domain match. To validate a model in the frequency domain, a technique called the frequency response is used.

The frequency response is a system's response to sinusoidal inputs [2]. In the frequency response of a vehicle, there is a distinctive phenomenon whose characteristic is similar to that of a notch filter, and little has been known about the cause of this notch. The notches are consistently seen in the work of others [1, 3, 4, 5, 6, 7, 8, 9, 10, 11, 12, 13, 14] that conducted the frequency responses on various kinds of vehicles. High-order or multi-body vehicle dynamic simulations such as Vehicle Dynamics Analysis Non-Linear (VDANL) [4, 6, 10], Improved Digital Simulation, Fully Comprehensive (IDSFC) [4], or CarSim, can reproduce this notch characteristic; however, a low-order vehicle dynamic model explaining the cause of this is lacking. This work is the first effort that tries to understand what the source of this notch is by using a low-order vehicle dynamic model.

The remainder of the paper is organized as follows: Section 2 presents two types of low-order linear vehicle dynamic models: the typical “bicycle model” and the newly proposed “roll dynamic model”. Section 3 gives an explanation on a vehicle system used to validate the fidelity of the proposed vehicle models. The testing procedures and experimental results are given in Section 4. Conclusions then summarize the main points of this paper.

2. Low-Order Vehicle Dynamic Modeling

In this section, two types of low-order linear vehicle dynamic models are developed: an in-plane vehicle dynamic model and an out-of-plane vehicle dynamic model. The in-plane vehicle dynamic model, also known as the two-degree-of-freedom model or the bicycle model [15], is a relatively simple model that describes vehicle planar dynamic characteristics by considering only lateral and yaw dynamics. This model is a well-known standard for studies of vehicle dynamics; however, it does not provide an understanding of vehicle's roll characteristics. To describe the vehicle's roll characteristics, the out-of-plane vehicle dynamic model is developed by modification of the in-plane dynamic model. The convention of the coordinates [16] and the sequence of coordinate rotations [17] used in this section are defined by the Society of Automotive Engineers (SAE).

2.1 In-Plane Vehicle Dynamic Model: the Bicycle Model

The derivation of the in-plane vehicle dynamic model is elaborated in this section. The nomenclature used in the formulation process is indicated in Fig. 1 and Table 1.

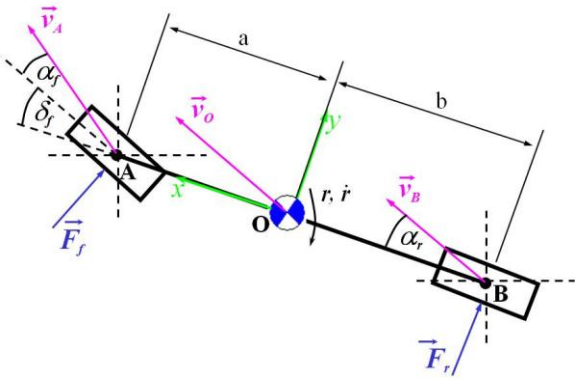

Fig. 1 Free-body diagram of bicycle model derived in body-fixed coordinates

Assumptions [18] are made to aid the derivation process, and, based on these assumptions, a four-wheeled vehicle can be assumed to be well-represented by a bicycle-like vehicle (Fig. 1) from which it derives its name, the bicycle model. The front and rear tire forces are assumed to be linear. In the free-body diagram,

point O is the center of gravity of the vehicle to which the coordinates xyz are attached.

Table 1 Nomenclature used in derivation of bicycle model

Symbol	Definition	Symbol	Definition
m	Vehicle mass	r	Yaw rate
I_{zz}	Z-axis mass moment of inertia about CG	F_f	Front tire force
		F_r	Rear tire force
a	Distance from CG to front axle along the x-axis	$C_{\alpha f}$	Front cornering stiffness
		$C_{\alpha r}$	Rear cornering stiffness
b	Distance from CG to rear axle along the x-axis	α_f	Front slip angle
		α_r	Rear slip angle
U	Longitudinal velocity at CG	δ_f	Front steering angle
V	Lateral velocity at CG		

From the free-body diagram in Fig. 1, the equations of motion for the bicycle model can be obtained directly by summing forces in the y-direction and moments in the z-direction. The force and moment equations respectively are:

$$C_{\alpha f}\left(\frac{V+ar}{U}-\delta_f\right)+C_{\alpha r}\left(\frac{V-br}{U}\right)=m(\dot{V}+Ur) \quad (1)$$

$$aC_{\alpha f}\left(\frac{V+ar}{U}-\delta_f\right)-bC_{\alpha r}\left(\frac{V-br}{U}\right)=I_{zz}\dot{r} \quad (2)$$

The above equations can be rewritten in the state-space form as:

$$\begin{aligned}\dot{\mathbf{x}}_1 &= \mathbf{A}_1\mathbf{x}_1+\mathbf{B}_1\mathbf{u}_1\\ \mathbf{y}_1 &= \mathbf{C}_1\mathbf{x}_1+\mathbf{D}_1\mathbf{u}_1\end{aligned} \quad (3)$$

where

$$\mathbf{x}_1=\begin{bmatrix} V & r\end{bmatrix}^T, \mathbf{u}_1=\delta_f$$

$$\mathbf{A}_1=\begin{bmatrix} \frac{C_{\alpha f}+C_{\alpha r}}{mU} & \frac{aC_{\alpha f}-bC_{\alpha r}}{mU}-U \\ \frac{aC_{\alpha f}-bC_{\alpha r}}{I_{zz}U} & \frac{a^2C_{\alpha f}+b^2C_{\alpha r}}{I_{zz}U}\end{bmatrix}$$

$$\mathbf{B}_1=\begin{bmatrix}\frac{-C_{\alpha f}}{m}\\ \frac{-aC_{\alpha f}}{I_{zz}}\end{bmatrix}, \mathbf{C}_1=\begin{bmatrix}1 & 0\\ 0 & 1\end{bmatrix}, \mathbf{D}_1=\begin{bmatrix}0\\0\end{bmatrix}$$

2.2 Out-Of-Plane Vehicle Dynamic Model: the Roll Dynamic Model

An out-of-plane vehicle dynamic model is derived in this section. The vehicle model discussed here is expanded from the previous section by including roll dynamics. This addition enhances the accuracy of the vehicle dynamic model in predicting roll characteristics of the vehicle and in understanding the effects of the vehicle's suspension. The nomenclature used in the development process is listed in Figs. 2 and 3, and Table 2.

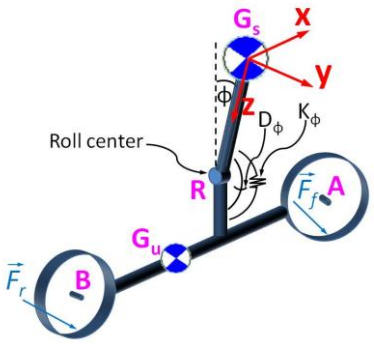

Fig. 2 Free-body diagram of roll dynamic model derived in body-fixed coordinates

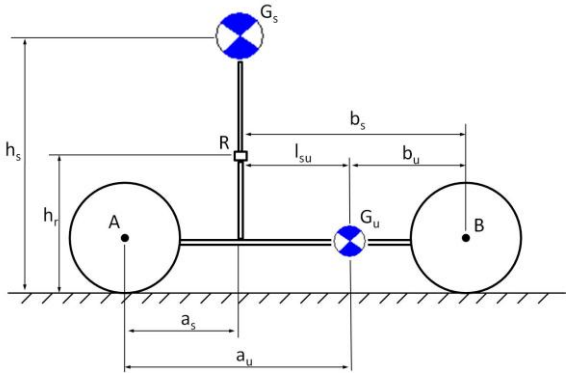

Fig. 3 Parameters associated with roll dynamic model

As in the case of bicycle model, assumptions [18] are made to simplify the complexity of a vehicle system and the associated mathematics in the derivation process. Based on the assumptions, the out-of-plane vehicle dynamic model, hereafter called

the roll dynamic model, is considered as an inverted pendulum connected to a moving cart as illustrated in Fig. 2. Consistent with the work of others [19, 20, 21, 22], the model is composed of two parts: a sprung mass G_s and an unsprung mass G_u. However, there is a slight difference in the configuration of the model proposed in this work and the others. In this work, the center of gravity of the sprung mass is not assumed to be in the same vertical plane as that of the unsprung mass.

The sprung mass is a mass that sits on a vehicle's suspension, and the remainder of the vehicle mass is the unsprung mass. Both the sprung and unsprung masses are linked together at a point called the roll center (point R). The roll center is a revolute joint that allows rotation only in the roll direction. The masses are supported by a torsional spring K_ϕ and a torsional damper D_ϕ. The torsional spring and torsional damper are assumed to simulate the vehicle's suspensions; additionally, this simplifies difficulties pertaining to the suspensions' kinematics and dynamics. The coordinates xyz are fixed to the center of gravity of the sprung mass (G_s).

Illustrated in Fig. 2, the free-body diagrams together with the Newton-Euler mechanics allow the derivation of the y-axis force equation, x-axis moment equation, and z-axis moment equation as follows:

$$m\dot{V} - m_u h_{sr}\dot{p}_s - m_u l_{su}\dot{r} = \left(\frac{C_{\alpha f} + C_{\alpha r}}{U}\right) V - h_{sr}\left(\frac{C_{\alpha f} + C_{\alpha r}}{U}\right) p_s + \left(\frac{a_s C_{\alpha f} - b_s C_{\alpha r}}{U} - mU\right) r - C_{\alpha f}\delta_f \quad (4)$$

Table 2 Nomenclature used in derivation of roll dynamic model

Symbol	Definition	Symbol	Definition
m	Total vehicle mass	h_s	Height from CG of sprung mass from ground
m_s	Sprung mass	h_r	Height from roll center from ground
m_u	Unsprung mass	U	Longitudinal velocity at CG of sprung mass in sprung mass's coordinates
I_{xxs}	X-axis mass moment of inertia about CG of sprung mass	V	Lateral velocity at CG of sprung mass in sprung mass's coordinate
I_{zz}	Z-axis mass moment of inertia about CG of total vehicle	φ	Roll angle of sprung mass
		p_s	Roll rate of sprung mass
I_{xzs}	Mass product of inertia about CG of sprung mass	r	Yaw rate
		F_f	Front tire force
a_s	Distance from CG of sprung mass to front axle along the x-axis	F_r	Rear tire force
		$C_{\alpha f}$	Front cornering stiffness
b_s	Distance from CG of sprung mass to rear axle along the x-axis	$C_{\alpha r}$	Rear cornering stiffness
		α_f	Front slip angle
a_u	Distance from CG of unsprung mass to front axle along the x-axis	α_r	Rear slip angle
		δ_f	Front steering angle
b_u	Distance from CG of unsprung mass to rear axle along the x-axis	$K\varphi$	Roll stiffness
		$D\varphi$	Roll damping coefficient
l_{su}	Distance from CG of sprung mass to CG of unsprung mass	g	Gravitational acceleration

$$m_s h_{sr}\dot{V} + I_{xx_s}\dot{p}_s - I_{xz_s}\dot{r} = (m_s g h_{sr} - K_\phi)\phi - D_\phi p_s - m_s h_{sr} U r \quad (5)$$

$$(m_u l_{su} + m_s h_{sr})\dot{V} - (I_{xz_s} + m_u l_{su} h_{sr})\dot{p}_s + (I_{zz} - m_u l_{su}^2)\dot{r} = \left(\frac{a_s C_{\alpha f} - b_s C_{\alpha r}}{U}\right) V - h_{sr}\left(\frac{a_s C_{\alpha f} - b_s C_{\alpha r}}{U}\right) p_s + \left[\frac{a_s^2 C_{\alpha f} + b_s^2 C_{\alpha r}}{U} - (m_u l_{su} + m_s h_{sr})U\right] r - a_s C_{\alpha f}\delta_f \quad (6)$$

where $h_{sr} = h_s - h_r$. These equations may be rewritten in a mass-damper-spring form as:

$$\mathbf{M}\dot{\mathbf{x}}_2 + \mathbf{N}\mathbf{x}_2 = \mathbf{F}\delta_f \quad (7)$$

where

$$\mathbf{x}_2 = \begin{bmatrix} V & \phi & p_s & r \end{bmatrix}^T$$

$$\mathbf{M} = \begin{bmatrix} m & 0 & -m_u h_{sr} & -m_u l_{su} \\ 0 & 1 & 0 & 0 \\ m_s h_{sr} & 0 & I_{xz_s} & -I_{xz_s} \\ (m_u l_{su} + m_s h_{sr}) & 0 & -(I_{xz_s} + m_u l_{su} h_{sr}) & (I_{zz} - m_u l_{su}^2) \end{bmatrix}$$

$$\mathbf{N} = -\begin{bmatrix} \left(\frac{C_{\alpha f} + C_{\alpha r}}{U}\right) & 0 & -h_{sr}\left(\frac{C_{\alpha f} + C_{\alpha r}}{U}\right) & \left(\frac{a_s C_{\alpha f} - b_s C_{\alpha r}}{U}\right) - mU \\ 0 & 0 & 1 & 0 \\ 0 & (m_s g h_{sr} - K_\phi) & -D_\phi & -m_s h_{sr} U \\ \left(\frac{a_s C_{\alpha f} - b_s C_{\alpha r}}{U}\right) & 0 & -h_{sr}\left(\frac{a_s C_{\alpha f} - b_s C_{\alpha r}}{U}\right) & N_{44} \end{bmatrix}$$

$$N_{44} = \left[\frac{a_s^2 C_{\alpha f} + b_s^2 C_{\alpha r}}{U} - (m_u l_{su} + m_s h_{sr})U\right]$$

$$\mathbf{F} = \begin{bmatrix} -C_{\alpha f} & 0 & 0 & -a_s C_{\alpha f} \end{bmatrix}^T$$

Further, from the mass-damper-spring form, the equations of motion can be represented in a state-space form:

$$\dot{\mathbf{x}}_2 = \mathbf{A}_2\mathbf{x}_2 + \mathbf{B}_2\mathbf{u}_2$$
$$\mathbf{y}_2 = \mathbf{C}_2\mathbf{x}_2 + \mathbf{D}_2\mathbf{u}_2 \quad (8)$$

where $\mathbf{A}_2 = -\mathbf{M}^{-1}\mathbf{N}$, $\mathbf{B}_2 = \mathbf{M}^{-1}\mathbf{F}$, $\mathbf{C}_2 = \mathbf{I}_{4\times4}$, $\mathbf{D}_2 = 0$, $\mathbf{u}_2 = \delta_f$, and $\mathbf{I}_{4\times4}$ is a four-by-four identity matrix.

3. Experimental Setup

This section provides a detailed description of the system that performs experiments to determine the accuracy of the vehicle models. The test vehicle is a 1989 GMC 2500 pick-up truck shown in Fig. 4. The truck is equipped with a Global Positioning System (GPS) and an Inertial Measurement Unit (IMU) to collect essential vehicle states. A string potentiometer is attached to a steering rack to obtain the front road-wheel steering angle. The string potentiometer is paired with a microcontroller (Arduino) to convert an output signal of the potentiometer from analog to digital. All sensors on the truck communicate with a host computer through a TCP/IP network. The computer runs QuaRC, which is a real-time data-acquisition/control software that seamlessly integrates with MATLAB/Simulink, to collect data streaming from the sensors.

Fig. 4 Test truck: 1989 GMC 2500

4. Results

The experiments were performed at the Thomas D. Larson Pennsylvania Transportation Institute's test track. The main variables of interest during these tests are lateral velocity, yaw rate, roll rate, and front road-wheel steering angle. The physical properties of the test truck used in the models are summarized in Table 3. The procedures and techniques to obtain these properties can be found in [18].

Table 3 Parameters of test truck

Symbol	Value	Unit	Symbol	Value	Unit
m	2279	kg	m_u	299	kg
m_s	1980	kg	a	1.390	m
b	1.964	m	a_u	2.042	m
b_u	1.312	m	a_s	1.358	m
b_s	1.996	m	h_s	0.882	m
h_r	0.5	m	I_{xx}	854	kg·m^2
I_{zz}	5411	kg·m^2	I_{xzs}	0	kg·m^2
$C_{\alpha f}$	-75709	N/rad	$C_{\alpha r}$	-83686	N/rad
K_φ	71177	N·m/rad	D_φ	2000	N·m·s/rad

The truck was driven at the relatively constant longitudinal speed of 11.18 m/s (25

mph) on the straight portion of the test track. The fidelity of the vehicle models was evaluated by measuring the frequency response of the vehicle. To obtain the frequency responses, the truck was excited by a series of sinusoidal steering inputs. The frequency of the sine-wave inputs ranged from 0.15 Hz to 3.47 Hz, and the response for each individual frequency was recorded. The frequency responses of the experimental data were created by using a technique called the correlation frequency response analysis [23, 24]. The frequency characteristics of the test vehicle are shown in Figs. 5, 6, and 7. Fig. 5 illustrates the frequency response of the lateral velocity of the truck for different frequencies of the front steering input. Similarly, the frequency responses corresponding to the yaw rate and the roll rate are shown in Figs. 6 and 7, respectively.

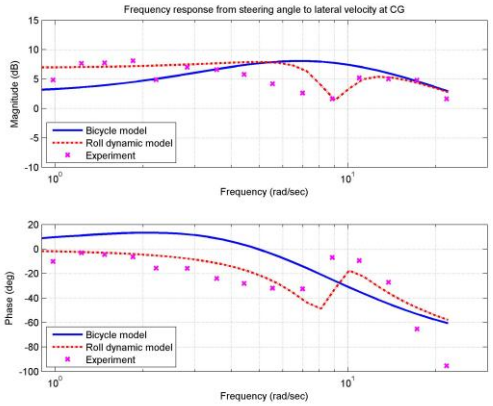

Fig. 5 Frequency response of the truck compared to the bicycle model and the roll dynamic model from front steering angle to lateral velocity

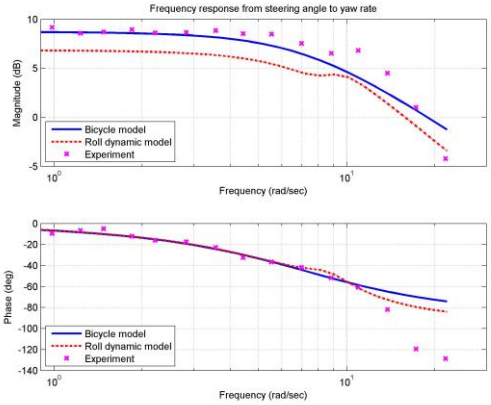

Fig. 6 Frequency response of the truck compared to the bicycle model and the roll dynamic model from front steering angle to yaw rate.

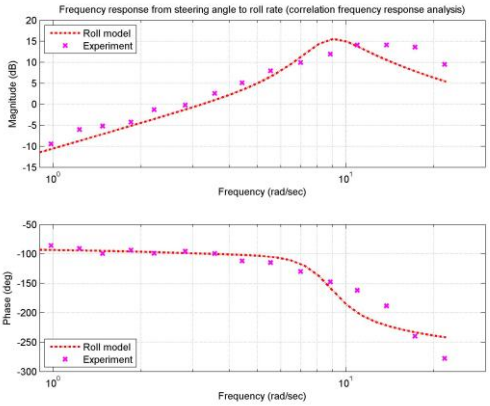

Fig. 7 Frequency response of the truck compared to the roll dynamic model from front steering angle to roll rate

In all of these figures, the experimental frequency responses are compared to those determined from the bicycle model and the roll dynamic model, which are respectively denoted by a solid blue line and a dash-dot red line. The top section of the plots is the magnitude plot, and the lower section is the phase plot. From the above results, one can see that the frequency responses of the vehicle models, especially those of the roll dynamic model, match with the experimental results really well. It is obvious that the bicycle model is not capable of adequately describing the dynamics of the

vehicle. Further, by including the roll dynamics, particularly the dynamics of the suspension, the roll model significantly improves the match to the experimental data. The roll model can even predict the notches seen in the frequency responses. From this, it can be inferred that the notches are caused by the dynamics of the vehicle suspension.

5. Conclusions

In this paper, two low-order linear vehicle dynamic models have been introduced. One is the well-known bicycle model, and the other is the newly proposed roll dynamic model. The fidelity of the models was evaluated with the experimental frequency characteristics of a vehicle. By comparing the experimental frequency responses with those obtained from the models, one can see that the standard bicycle model cannot adequately explain the dynamics of the vehicle. By adding one more degree-of-freedom to the bicycle model (roll mode) to represent the vehicle suspension, the proposed roll model substantially betters the match to the experimental responses. The roll model can further capture the notch phenomenon seen in the frequency characteristics, which none of the previous work can do with low-order vehicle models.

6. References

[1] Heydinger, G.J., Garrott, W.R., Chrstos, J.P., and Guenther, D.A. (1990). A methodology for validating vehicle dynamics simulations, *SAE Tech. Paper Series*, no. 900128.

[2] Franklin, G.F., Powell, J.D., and Emami-Naeini, A. (2002). *Feedback Control of Dynamic Systems,* 4th edition, Prentice-Hall, Upper Saddle River, NJ, USA.

[3] Allen, R.W., Szostak, H.T., Rosenthal, T.J., and Klyde, D.H. (1990). Field Testing and Computer Simulation Analysis of Ground Vehicle Dynamics Stability, *SAE Tech. Paper Series*, no. 900127.

[4] Heydinger, G.J. (1990). Improved Simulation and Validation of Road Vehicle Handling Dynamics, Ph.D. Dissertation, The Ohio State University.

[5] Allen, R.W., Szostak, H.T., Klyde, D.H., Owens, K.J., and Rosenthal, T.J. (1992). Validation of Ground Vehicle Computer Simulations Developed for Dynamic Stability Analysis, *SAE Tech. Paper Series*, no. 920054.

[6] Allen, R.W., Szostak, H.T., Klyde, D.H., Rosenthal, T.J., and Owens, K.J. (1992). Vehicle Dynamic Stability and Rollover, DOT HS 807 956.

[7] Allen, R.W., Rosenthal, T.J., Klyde, D.H., and Chrstos, J.P. (1992). Vehicle and Tire Modeling for Dynamic Analysis and Real Time Simulation, *SAE Tech. Paper Series*, no. 2000-01-1620.

[8] Demerly, J.D., and Youcef-Toumi, K. (2000). Non-Linear Analysis of Vehicle Dynamics (NAVDyn): A Reducd Order Model for Vehicle Handling Analysis, *SAE Tech. Paper Series*, no. 2000-01-1621.

[9] Salaani, M.K., Grygier, P.A., and Heydinger G.J. (2000). Model Validation of the 1998 Chevrolet Malibu for the National Advanced Driving Simulator, *SAE Tech. Paper Series*, no. 2001-01-0141.

[10] Allen, R.W., Chrstos, J.P., Howe, G., Klyde, D.H., and Rosenthal, T.J. (1992). Validation of a Non-Linear Vehicle Dynamic Simulation for Limit Handling, *Proc. Instn. Mech. Engrs., Part D: J.*

Automobile Engineering, vol. 216(4), pp. 319-327.

[11] Brusa, E., Velardocchia, M., Danesin D., Krief, P., and Suraci E. (2000). Modelling Vehicle Dynamics for Virtual Experimentation, Road Test Suppoting and Dynamic Control, *SAE Tech. Paper Series*, no. 2002-01-0815.

[12] Hamblin, B.C., Martini, R.D., Cameron, J.T., and Brennan, S.N. (2006), Low-Order Modeling of Vehicle Roll Dynamics, paper presented in *the 2006 American Control Conference*, Minneapolis, MN, USA.

[13] Laws, S.M., Gadda, C.D., and Gerdes, J.C. (2006), Frequency Characteristics of Vehicle Handling Modeling and Experimental Validation of Yaw, Sideslip and Roll Models to 8 {Hz}, paper presented in *the 8th Int. Symp. On Advanced Vehicle Control: AVEC2006*, Taipei, Taiwan.

[14] Brennan, S.N., and Hamblin, B.C. (2007), Lessons Learned from Matching Experimental Data to Low-Order Models of Vehicle Yaw, Sideslip, and Roll Behaviour, paper presented in *the 2007 ASME Int. Mechanical Engineering Congress and Exposition*, Seattle, WA, USA.

[15] Rajamani, R. (2006). *Vehicle Dynamics and Control*, Springer Science+Bussiness Media, Inc., New York, NY, USA.

[16] Milliken, W. F., and Milliken D.L. (1995). Race Car *Vehicle Dynamics*, Society of Automotive Engineers, Inc., Warrendale, PA, USA.

[17] Society of Automotive Engineers, Inc. (1976), Vehicle Dynamics Terminology—SAE J670e, Technical Report

[18] Lapapong, S. (2010). Vehicle Rollover Prediction for Banked Surfaces, Ph.D. Dissertation, The Pennsylvania State University.

[19] Mammar, S., Baghdassarian, V.B., and Nouveliere L. (1999), Speed Scheduled Lateral Vehicle Control, paper presented in *the 1999 IEEE/IEEJ/JSAI Int. Conf. on Intelligent Transportation Systems*, Tokyo, Japan.

[20] Carlson, C.R., and Gerdes, J.C. (2007), Optimal Rollover Prevention with Steer By Wire and Differential Braking, paper presented in *the 2003 ASME Int. Mechanical Engineering Congress and Exposition*, Washington, DC, USA.

[21] Takano, S., Nagai, M.., Taniguchi, T., and Hatano, T. (2003). Study on Vehicle Dynamics for Improving Roll Stability, *JSAE Review,* vol. 24(2), pp. 149-156.

[22] Kim, H.-J., and Park, Y.-P. (2004). Investigation of Robust Roll Motion Control Considering Varying Speed and Actuator Dynamics, *Mechatronics,* vol. 14(1), pp. 35-54.

[23] Wellstead, P.E. (2003). Frequency Response Analysis, Technical Report No. 10, Solartron Instruments, Hampshire, UK.

[24] Laubwald, E., and Readman M. Frequency Response Analysis, Technical Report, Control-Ststems-Principles.co.uk, Cheshire, UK.